Supplemental Information

Supplemental Methods

CDNA Constructs and Vectors

Full length FLAG tagged murine HoxA9 (1) (99% homology to human) was PCR amplified from PRC-CMV-FLAG HoxA9 (gift, C.Largman, UCSF, San Francisco, CA.) using forward T7 and reverse *mur* HoxA9-*Not1* 5' GAT CGC GGC CGC TAA GCC CAA ATG GCA TCA 3' primers and subsequently subcloned into the *SalI-NotI* vector fragment of the Hermes HRS puro IRES eGFP retroviral plasmid (2) (gift, H.Blau, Stanford University, Stanford, CA). The *SalI-NotI* FLAG tagged HoxA9 fragment from Hermes HRS puro Hox9 IRES eGFP was replaced with an HA tagged murine HoxA9 PCR product amplified from pHRS-puro-Flag-HoxA9-ires-eGFP using forward primer *BamH1-Sal1*-HA-*mur*-HoxA9 5' GCG GGA TCC GTC GAC CCA CCA TGG GCT ACC CCT ACG ACG TGC CCG ACT ACG CCA TGG CCA CCA CCG GGG CCC T 3' and reverse primer *mur* HoxA9-*Not1*. pcDNA3.1 HA HoxA9 was derived by cloning the HA tagged murine HoxA9 PCR product into the *BamHI-NotI* vector fragment of pcDNA3.1 (Invitrogen). Full length wild-type HA tagged BRCA1 (3) (gift, F.Rauscher, Wistar Institute, Philadelphia, PA) in the pcDNA3.1 vector was partially digested with *BamHI-KpnI* or *KpnI-NotI* to obtain the HA tagged 5' end or 3' end of BRCA1. Hermes HRS puro IRES eGFP was partially digested with *NotI-XbaI* to obtain the IRES-eGFP fragment. All three fragments were ligated into the Hermes HRS puro IRES eGFP *BamHI-NotI* vector fragment. pcDNA3.1 HA tagged BRCA1 Δ exon 11b (3) (gift, F.Rauscher, Wistar Institute, Philadelphia, PA) was digested with *BamHI-NotI* and cloned into the *BamHI-XbaI* vector fragment of Hermes HRS neo IRES eGFP together

with the *NotI-XbaI* IRES-eGFP fragment (described above). The pGL2 BRCA1 luciferase plasmid (4) (gift, L.A. Chodosh, UPENN, Philadelphia, PA) was used directly. The pGL2 BRCA1 luciferase mutants were generated by PCR amplification using *Pfu* turbo polymerase (Stratagene) and the following primer pairs: Δ-223 to +44 forward 5' GCG CGA TAT CTG CCT GCC CTC TAG CCT CTA CTC TTC 3' and Δ-223 to +44 reverse 5'GCG CGA TAT CCG GGG GAC AGG CTG TGG GGT TTC TCA 3', Δ-221 to -218 forward 5' GCG CGA TAT CGC AAA CTC AGG TAG AAT TCT TCC TC 3' and Δ-221 to -218 reverse 5' GCG CGA TAT CCT GCC CTC TAG CCT CTA CTC TTC CAG 3', Δ-175 to -172 forward 5' GCG CGA TAT CTC ATC CGG GGG CAG ACT GGG TGG CCA 3' and Δ-175 to -172 reverse 5'GCG CGA TAT CAA GAG ACG GAA GAG GAA GAA TTC TAC 3', Δ –12 to -9 forward 5' GCG CGA TAT CGA TAA ATT AAA ACT GCG ACT GCG CGG 3' and Δ –12 to -9 reverse 5'GCG CGA TAT CGC GCT TTT CCG TTG CCA CGG AAA CCA 3'. pcDNA3.1-SEAP was generated by cloning the *EcoRI-XbaI* SEAP fragment from pGRE-SEAP (Clontech) into the *EcoRI-XbaI* vector fragment of pcDNA3.1-eGFP (Invitrogen). CMV-PBX1 was used directly (5). pcDNA3.1 HA-HoxA9 DNA binding mutant was generated by PCR amplification using *Pfu* turbo polymerase (Stratagene) and the following primer pair: 5'GGC AGG TCA AGA TCT GGT TCC AGA CCC GCA GGA TGA AAA TGA AGA AAA TCA 3' and 5'ATT TTC TTC ATT TTC ATC CTG CGG GTC TGG AAC CAG ATC TTG ACC TGC CTT TC 3'. HoxA10 cDNA (gift, H.J.Lawrence, UCSF, San Francisco, CA) was excised from pBluescript and subcloned into the EcoR1 restriction site of the pLXSN (Clontech) retroviral vector. Orientation was confirmed by Big Dye™ terminator analysis (PE Biosystems) at the UCSF Biomolecular Core facility. pLKO.1-puro-

luciferase shRNA and BRCA1 shRNA lentiviral plasmids were used directly (Sigma-Aldrich, MISSION^{TM} TRC-Hs1.0)(6). The following MISSION^{TM} human BRCA1 shRNA clones were screened: TRC0000039833 (#1), TRC0000039834 (#2), TRC0000039835 (#3), TRC0000039836 (#4), TRC0000039837 (#5). The following MISSION^{TM} murine HoxA9 shRNA clones were screened: TRCN0000012508 (#1), TRCN0000012509 (#2), TRCN0000012510 (#3), TRCN0000012511 (#4), TRCN0000012512 (#5). The pMD2.G and pCMVΔR8.91 packaging plasmids were used directly (gift, D.Trono, EPFL, Lausanne, Switzerland). All plasmids were confirmed by restriction and sequence analysis (7).

Lentiviral Infection

Lentiviral particles were produced, harvested, and used to infect target cells as previously described (8).

Expression Profiling

All experiments were performed in accordance with Institutional Review Board approval at the University of Pennsylvania. Dissected tissues from human breast tumor and adjacent " normal" tissue were rapidly homogenized using the Tissue Tearer^{TM} apparatus (BioSpec Products, Inc.) and log phase cultured breast cells were harvested and total RNA from samples was isolated and labeled, and cRNA was prepared, fragmented and hybridized to U95A arrays, essentially as recommended by the manufacturer (GeneChip^{TM} protocol, Affymetrix, Inc.). The microarrays were scanned and images were assessed for quality and normalization using GeneChip Analysis Suite 5.0

(Affymetrix, Inc.). Data from each microarray analysis was exported as a .DAT file into Rosetta Resolver^{TM} 3.0 (Rosetta Inpharmatics, Inc.) and statistically analyzed using 2D agglomerative clustering. Using this approach, expression data were clustered for similarity across experiments and experiments were clustered for similarity across genes. Probe set clusters detecting transcript level differences between normal and malignant tissue with $p \leq 0.01$ as calculated by Rosetta Resolver ^{TM} in at least four of five tumor/normal pairs were included in the list of genes that was significantly up- or down-regulated, using normal adjacent as the background sample. Thus up-regulated genes correspond to transcripts that are more highly expressed in tumor compared to normal tissue, and vice versa.

Multispectral image analysis.

Immunohistochemistry slides were examined using a Leica DMRA2 microscope (Leica Microsystems Inc.) equipped with plan apochromatic lenses. Fields containing tumor or normal tissues were imaged at 40X magnification through a liquid crystal filter using the Nuance Multispectral Imaging System (Cambridge Research and Instrumentation Inc.). The spectro-microscopic system is linked to a CCD camera and a PC. The MSI system was used at full chip resolution, without data binning. Spectral data was acquired from 420-720 nm in 20 nm increments. Spectral unmixing was accomplished by using Nuance software v1.42 using pure spectral libraries of individual chromogens (slides stained with only DAB, Fast red, or hematoxylin). Images were then evaluated for the presence of BRCA1, HoxA9 or both in normal epithelium or tumor cells using unmixed images from the Nuance system.

2D Growth Curves

50,000 cells in log phase growth were plated into fifteen 35 mm polystyrene tissue culture plastic dishes. Three dishes were trypsinized and counted every 24 hours for five consecutive days after they were initially plated. Data was plotted as time (days) versus average cell number and the growth rate was determined by calculating the slope of the line during exponential growth.

Bioinformatics Analysis

The mRNA expression levels for HoxA9 were analyzed from several independent cancer studies using Oncomine™ (www.oncomine.org) (9). Details of standard normalization methods and statistical calculations are provided on the Oncomine™ website.

Gene expression and clinical outcome information were obtained from two independent publicly available data sets (10-12). Clinical outcomes from the Pawitan study (12) was obtained from data published in the Ivshina study (11). In all cases, data for HoxA9 was culled from normalized expression data for each breast tumor sample, and patients were divided into quartiles based on HoxA9 expression. Each data set was analyzed separately. For the data from the van de Vijver study, distant metastasis was analyzed as first event only. If a patient developed a local recurrence, axillary recurrence, contra-lateral breast cancer, or a second primary cancer (except for non-melanoma skin cancer), she was censored at that time. Any distant metastasis after the first event was not analyzed, based on the theoretical possibility that the secondary cancers could be a source for distant metastases. An ipsalateral supra-clavicular recurrence was considered as first clinical evidence for metastatic disease for this analysis. Therefore, patients with

ipsalateral supra-clavicular recurrence were not censored. Patients were censored at last follow-up. Kaplan-Meier survival curves were generated using the software WINSTAT FOR EXCEL (R. Fitch Software), and p values were calculated by log-rank analysis. Multivariate analyses with Cox's proportional-hazards regression were performed on the expression levels of HoxA9 and clinicopathological variables provided in the NKI data set with SPSS 10.0 (SPSS), with patients stratified according to their local lymph node (LN) and estrogen receptor (ER) status, the molecular subtypes of breast cancer (13) and further grouped into quartiles based on the relative (untransformed) expression levels of HoxA9 (10). P-values less than 0.05 were considered significant.

Supplemental References

1. Shen, W.F., Rozenfeld, S., Kwong, A., Kom ves, L.G., Lawrence, H.J., and Largman, C. 1999. HOXA9 forms triple complexes with PBX2 and MEIS1 in myeloid cells. *Mol Cell Biol* 19:3051-3061.
2. Rossi, F.M., Guicherit, O.M., Spicher, A., Kringstein, A.M., Fatyol, K., Blakely, B.T., and Blau, H.M. 1998. Tetracycline-regulatable factors with distinct dimerization domains allow reversible growth inhibition by p16. *Nat Genet* 20:389-393.
3. Wilson, C.A., Payton, M.N., Elliott, G.S., Buaas, F.W., Cajulis, E.E., Grosshans, D., Ramos, L., Reese, D.M., Slamon, D.J., and Calzone, F.J. 1997. Differential subcellular localization, expression and biological toxicity of BRCA1 and the splice variant BRCA1-delta11b. *Oncogene* 14:1-16.
4. Thakur, S., and Croce, C.M. 1999. Positive regulation of the BRCA1 promoter. *J Biol Chem* 274:8837-8843.
5. Charboneau, A., East, L., Mulholland, N., Rohde, M., and Boudreau, N. 2005. Pbx1 is required for Hox D3-mediated angiogenesis. *Angiogenesis* 8:289-296.
6. Moffat, J., Grueneberg, D.A., Yang, X., Kim, S.Y., Kloepfer, A.M., Hinkle, G., Piqani, B., Eisenhaure, T.M., Luo, B., Grenier, J.K., et al. 2006. A lentiviral RNAi library for human and mouse genes applied to an arrayed viral high-content screen. *Cell* 124:1283-1298.
7. Yu, S.F., von Ruden, T., Kantoff, P.W., Garber, C., Seiberg, M., Ruther, U., Anderson, W.F., Wagner, E.F., and Gilboa, E. 1986. Self-inactivating retroviral vectors designed for transfer of whole genes into mammalian cells. *Proc Natl Acad Sci U S A* 83:3194-3198.
8. Zufferey, R., Dull, T., Mandel, R.J., Bukovsky, A., Quiroz, D., Naldini, L., and Trono, D. 1998. Self-inactivating lentivirus vector for safe and efficient in vivo gene delivery. *J Virol* 72:9873-9880.
9. Rhodes, D.R., Yu, J., Shanker, K., Deshpande, N., Varambally, R., Ghosh, D., Barrette, T., Pandey, A., and Chinnaiyan, A.M. 2004. ONCOMINE: a cancer microarray database and integrated data-mining platform. *Neoplasia* 6:1-6.
10. van de Vijver, M.J., He, Y.D., van't Veer, L.J., Dai, H., Hart, A.A., Voskuil, D.W., Schreiber, G.J., Peterse, J.L., Roberts, C., Marton, M.J., et al. 2002. A gene-expression signature as a predictor of survival in breast cancer. *N Engl J Med* 347:1999-2009.
11. Ivshina, A.V., George, J., Senko, O., Mow, B., Putti, T.C., Smeds, J., Lindahl, T., Pawitan, Y., Hall, P., Nordgren, H., et al. 2006. Genetic reclassification of histologic grade delineates new clinical subtypes of breast cancer. *Cancer Res* 66:10292-10301.
12. Pawitan, Y., Bjohle, J., Amler, L., Borg, A.L., Egyhazi, S., Hall, P., Han, X., Holmberg, L., Huang, F., Klaar, S., et al. 2005. Gene expression profiling spares early breast cancer patients from adjuvant therapy: derived and validated in two population-based cohorts. *Breast Cancer Res* 7:R953-964.
13. Sorlie, T., Perou, C.M., Tibshirani, R., Aas, T., Geisler, S., Johnsen, H., Hastie, T., Eisen, M.B., van de Rijn, M., Jeffrey, S.S., et al. 2001. Gene expression

patterns of breast carcinomas distinguish tumor subclasses with clinical implications. *Proc Natl Acad Sci U S A* 98:10869-10874.

14. Xu, C.F., Brown, M.A., Chambers, J.A., Griffiths, B., Nicolai, H., and Solomon, E. 1995. Distinct transcription start sites generate two forms of BRCA1 mRNA. *Hum Mol Genet* 4:2259-2264.

Supplemental Table 1

Tumor ID	1	2	3	4	5
Diagnosis*	IDC	IDC	IDC	IDC	IDC
Max. Diameter (cm)	2.6	4.9	1.9	1.5	2.0
Nuclear Grade	HIGH	HIGH	HIGH	HIGH	HIGH
Histologic Grade	HIGH	HIGH	HIGH	HIGH	HIGH
Estrogen Receptor Status	NEG	ND	NEG	NEG	NEG

*IDC-Infiltrating Ductal Carcinoma

Supplemental Table 1. Tumor characteristics of matched normal-tumor pairs analyzed by global expression profiling.

Supplemental Table 2

Fold Change[a]	Gene	Description
Transcripts upregulated in the tumor compared to the matched normal adjacent tissue in at least 4 out of 5 samples		
2.5	*PFN2*	Profilin 2
3.2	*TACSTD1*	Tumor-associated calcium signal transducer 1
3.2	*KRT7*	Keratin 7
3.5	*MTHFD2*	Mitochondrial methylene tetrahydrofolate dehydrogenase
3.7	*CCNB2*	Cyclin B2
6.1	*STAT1*	Signal transducer and activator of transcription 1
9.4	*COL11A1*	Collagen, type XI, alpha 1
11	*H2AFA*	H2A histone family, member A
12.9	*MUC1*	Mucin 1
48.6	*S100BPP*	S-100 calcium binding protein B
Transcripts downregulated in the tumor compared to the matched normal adjacent tissue in at least 4 out of 5 samples		
-2.5	*TGFBR2*	Transforming growth factor beta receptor 2
-2.8	*GAS1*	Growth arrest specific 1
-3.1	***HOXA4***	**Homeobox A4**
-3.1	*ID1*	Inhibitor of DNA binding 1
-3.5	*SEMA3C*	Semaphorin 3C
-3.7	*MEOX2*	Mesenchyme homeobox 2
-4.2	*PECAM1*	Platelet/endothelial cell adhesion molecule 1
-4.4	***HOXA9***	**Homeobox A9**
-6.1	*JAM3*	Junctional adhesion molecule 3
-6.5	*RAPGEF*	Rap1 guanine-nucleotide-exchange factor
-7.6	*VWF*	von Willebrand factor
-7.7	*ABC1*	ATP-binding cassette 1
-8.4	*DUSP1*	Dual specificity phosphatase 1
-9	*Col17A1*	Collagen, type XVII
-10.5	*CXCL12*	Chemokine ligand 12 (*SDF1*)
-11	*MEOX1*	Mesenchyme homeobox 1
-11.8	*AQP1*	Aquaporin 1
-13.9	*FHL1*	Four and a half LIM domains 1
-14.5	*ITGA7*	Integrin alpha 7
-21.4	*CLDN5*	Claudin 5
-23.4	*FABP4*	Fatty acid binding protein 4
-26.9	*CNN1*	Calponin 1, basic, smooth muscle
-28.5	*ADH1C*	Alcohol dehydrogenase 1C
-34.7	*CCR5*	Chemokine receptor 5
-45.2	*c-fos*	Fos proto-oncogene

[a] *p*-value ≤0.01

Supplemental Table 2. Select genes from a Rosetta-Resolver™ generated list of transcripts significantly altered in at least 4 out of 5 sets of matched tumor and normal adjacent tissue pairs.

Supplemental Table 3

Clinical parameters related to reduced HoxA9 mRNA levels in human breast cancers	n	*P* value	Reference
breast cancer vs. normal breast	47	**0.0000014**	Richardson, et al. Cancer Cell. 2006 Feb;9(2):121-32.
	10	**0.002**	Turashvili et al. BMC Cancer. 2007 Mar 27;7:55.
high grade breast cancers	278	**0.000091**	Bittner, et al. https://expo.intgen.org/expo/public/ 2005/01/15
	172	**0.006**	Soritrou et al. J Natl Cancer Inst. 2006 Feb 15;98(4):262-72.
	55	**0.018**	Ginestier et al. Clin Cancer Res. 2006 Aug 1;12(15):4533-44.
	249	**0.018**	Miller et al. Proc Natl Acad Sci U S A. 2005 Sep 20;102(38):13550-5.
	249	**0.023**	Ivshina et al. Cancer Res. 2006 Nov 1;66(21):10292-301.
	60	**0.03**	Ma et al. Cancer Cell. 2004 Jun;5(6):607-16.
high stage breasts cancers	244	**0.00047**	Bittner, et al. https://expo.intgen.org/expo/public/ 2005/01/15
tumors with complete response vs. residual disease	51	**0.002**	Hess et al. J Clin Oncol. 2006 Sep 10;24(26):4236-44.
tumors sensitive to docetaxel	24	**0.003**	Chang et al. Lancet. 2003 Aug 2;362(9381):362-9.
tumors with lymph node involvement (N3)	194	**0.005**	Bittner, et al. https://expo.intgen.org/expo/public/ 2005/01/15
large (T4) tumors	285	**0.021**	Bittner, et al. https://expo.intgen.org/expo/public/ 2005/01/15
tumors associated with distant metastasis	189	**0.03**	Desmedt et al. Clin Cancer Res. 2007 Jun 1;13(11):3207-14.
< 5 year survival	159	**0.038**	Pawitan et al. Breast Cancer Res. 2005;7(6):R953-64.

Supplemental Table 3. Clinical parameters related to reduced HoxA9 mRNA levels in human breast cancers.

Supplemental Table 4

Signal Log Ratio	Fold Change[a]	Gene	Description
Transcripts decreased after *HoxA9* induction			
-4.2	-17.6	*NBR2*	Next to BRCA1 gene 2
-4.0	-16.0	*TOM1*	Target of Myb1
-3.7	-13.7	*CDK5R1*	Regulatory subunit of cyclin-dependent kinase 5
-3.7	-13.7	*DMXL1*	DmX-Like 1 regulatory protein
-3.5	-12.3	*RENT2*	Nuclear export protein
Transcripts increased after *HoxA9* induction			
1.0	**+2.0**	***HoxA9***	**Homeobox domain protein A9**
1.0	+2.0	*CDK9*	Cyclin-dependent protein kinase 9
1.3	+2.5	*MYB*	MYB oncogene
1.5	+2.8	*NDRG2*	N-myc downstream-regulated gene2
1.9	+3.7	*CSN1*	Alpha S1-casein
1.9	+3.7	*ACVR2*	Activin 2 (TGF-beta superfamily)
2.2	+4.6	*CDK8*	Cyclin-dependent protein kinase 8
2.4	+5.3	*MUC5B*	Mucin 5B
2.5	+5.7	*RAP2A*	RAS-related protein 2A
2.6	+6.0	*PCDH9*	Protocadherin 9
2.7	+7.3	*PRKCBP2*	Protein kinase C-binding protein RACK17
2.9	+8.4	*PTEN*	Dual specificity phospatase
3.1	+9.6	*WNT10B*	Wingless-type MMTV integration site 10B
3.1	+9.6	*BMP1*	Bone morphogenetic protein 1
3.2	+10.2	*COL1A2*	Collagen alpha-2 type I
3.3	+10.9	*NEO1*	Member of NCAM cell adhesion family
3.3	+10.9	*MMP1*	Matrix metalloproteinase 1
4.1	+16.8	*MUC1*	Mucin 1
4.1	+16.8	*ERBB3*	Epidermal growth factor receptor 3 (HER3)
4.6	+21.1	*BRCA1*	**BReast CAncer-related gene 1**

[a]Fold change is expressed as $\log^2$ of the signal log ratio calculated by Affymetrix Analysis Suite 5.0
p-values ≤0.001

Supplemental Table 4. Selected gene expression differences following HoxA9 induction in MDA-MB-231 cells.

Supplemental Legends

Supplemental Figure S1. HoxA9 expression is reduced in ER/PR positive and negative breast tumors. Quantitative RT-PCR showing levels of HoxA9 mRNA in normal human mammary tissue compared to levels in ER/PR negative and positive human mammary tumor tissue. ***$p<0.001$ compared to normal mammary tissue (normal: n=16, ER+/PR+ tumor: n=24, ER-/PR- tumor: n=23).

Supplemental Figure S2. Levels of HoxA9 protein upon re-expression in breast tumor cell lines. Immunoblot showing level of expressed transgenic HoxA9 protein attained in MDA-231 (left) and T4-2 (right) breast tumor cells compared to cells expressing a vector control.

Supplemental Figure S3. Tetracycline regulated HoxA9 re-expression in breast tumor cell lines. Epi-fluorescence microscopy images of breast tumor cells (MDA-231, A & B; T4-2, A' & B') stably re-expressing retroviral HoxA9 bi-cistronically with EGFP, showing transgene expression in the absence (B & B') and its loss (A & A') upon tetracycline exposure (0.5 mg/ml; 72 hours). Insert: Phase contrast microscopy images of A, A', B & B' indicating similar cell numbers were used under all experimental conditions. Bars equal 50 mm.

Supplemental Figure S4. HoxA9 expression does not alter proliferation on 2D tissue culture plastic. Growth curves of MDA-231 (black lines) and T4-2 (gray lines) breast

tumor cells expressing a vector control (squares) or HoxA9 (circles) demonstrating that exogenous HoxA9 expression does not alter 2D proliferation (n=3).

Supplemental Figure S5. HoxA9 re-expression phenotypically reverts breast tumor cells. Bar graphs quantifying the tumor colony organization of T4-2 cells grown within a 3D reconstituted basement membrane for 10-12 days. Cell-cell junction integrity (left graph) assessed by β-catenin cell-cell localization and continuity of staining. Basal polarity (right graph) assessed by basal localization and continuity of β4 integrin staining. ***P<0.001.

Supplemental Figure S6. Exogenous HoxA10 expression in MDA-231 breast tumor cells. Semi-Q-PCR gel (left) and immunoblot (right) showing levels of HoxA10 RNA and protein achieved upon re-expression in MDA-231 breast tumor cells. Lack of chemiluminescent signal in HoxD10 lysates demonstrates the specificity of the HoxA10 antibody.

Supplemental Figure S7. HoxA10 expression in mammary epithelial tumor cells does not reduce rBM colony growth. Phase contrast images of MDA-231 mammary epithelial tumor cells expressing a vector control, HoxA9 or HoxA10 transgene showing that growth inhibition within a 3D rBM is HoxA9 specific. Bar=50 μm.

Supplemental Figure S8. Mutational analysis of putative HoxA9 binding sites. Luciferase reporter analysis showing continued responsiveness of BRCA1 promoter

constructs to addition of wild-type HoxA9 when single putative HoxA9 binding sites are deleted (Δ-221 to -218, Δ-175 to -172, and Δ-12 to -9) that is comparable to the activation of the full length BRCA1 promoter construct (compare gray bars). Data are normalized to matched vector control (black bars). Negative numbers refer to basepairs upstream of the BRCA1 transcription start site (14).

Supplemental Figure S9. shRNA mediated HoxA9 knockdown. Q-RT-PCR analysis of HoxA9 RNA levels in nonmalignant MCF10A mammary epithelial cells expressing a luciferase control shRNA construct (Luc) or a HoxA9 shRNA clone.

Supplemental Figure S10. The BRCA1 Δexon11b mutant functions as a dominant negative mutant. Immunoblot demonstrating that exogenous expression of BRCA1 Δexon11b (140KDa) in nonmalignant MCF10A cells completely abrogates levels of wild-type BRCA1 (220KDa) suggesting the BRCA1 mutant functions as a dominant negative.

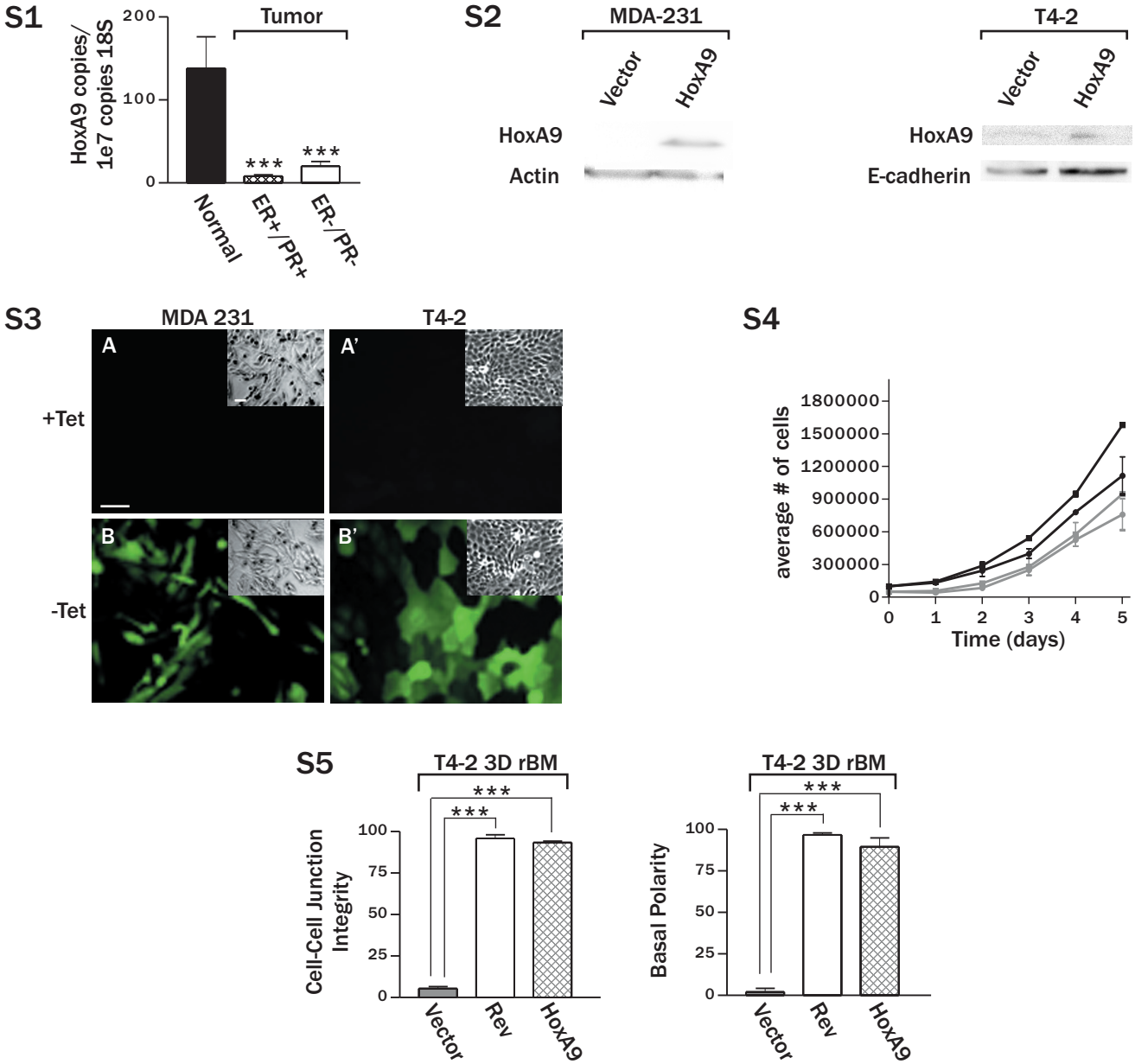

Supplemental Figure S1. HoxA9 expression is reduced in ER/PR positive and negative breast tumors. Quantitative RT-PCR showing levels of HoxA9 mRNA in normal human mammary tissue compared to levels in ER/PR negative and positive human mammary tumor tissue. ***p<0.001 compared to normal mammary tissue (normal: n=16, ER+/PR+ tumor: n=24, ER-/PR- tumor: n=23).

Supplemental Figure S2. Levels of HoxA9 protein upon re-expression in breast tumor cell lines. Immunoblot showing level of expressed transgenic HoxA9 protein attained in MDA-231 (left) and T4-2 (right) breast tumor cells compared to cells expressing a vector control.

Supplemental Figure S3. Tetracycline regulated HoxA9 re-expression in breast tumor cell lines. Epi-fluorescence microscopy images of breast tumor cells (MDA-231, A & B; T4-2, A' & B') stably re-expressing retroviral HoxA9 bi-cistronically with EGFP, showing transgene expression in the absence (B & B') and its loss (A & A') upon tetracycline exposure (0.5 μg/ml; 72 hours). Insert: Phase contrast microscopy images of A, A', B & B' indicating similar cell numbers were used under all experimental conditions. Bars equal 50 μm.

Supplemental Figure S4. HoxA9 expression does not alter proliferation on 2D tissue culture plastic. Growth curves of MDA-231 (black lines) and T4-2 (gray lines) breast tumor cells expressing a vector control (squares) or HoxA9 (circles) demonstrating that exogenous HoxA9 expression does not alter 2D proliferation (n=3).

Supplemental Figure S5. HoxA9 re-expression phenotypically reverts breast tumor cells. Bar graphs quantifying the tumor colony organization of T4-2 cells grown within a 3D reconstituted basement membrane for 10-12 days. Cell-cell junction integrity (left graph) assessed by β-catenin cell-cell localization and continuity of staining. Basal polarity (right graph) assessed by basal localization and continuity of β4 integrin staining. ***P<0.001.

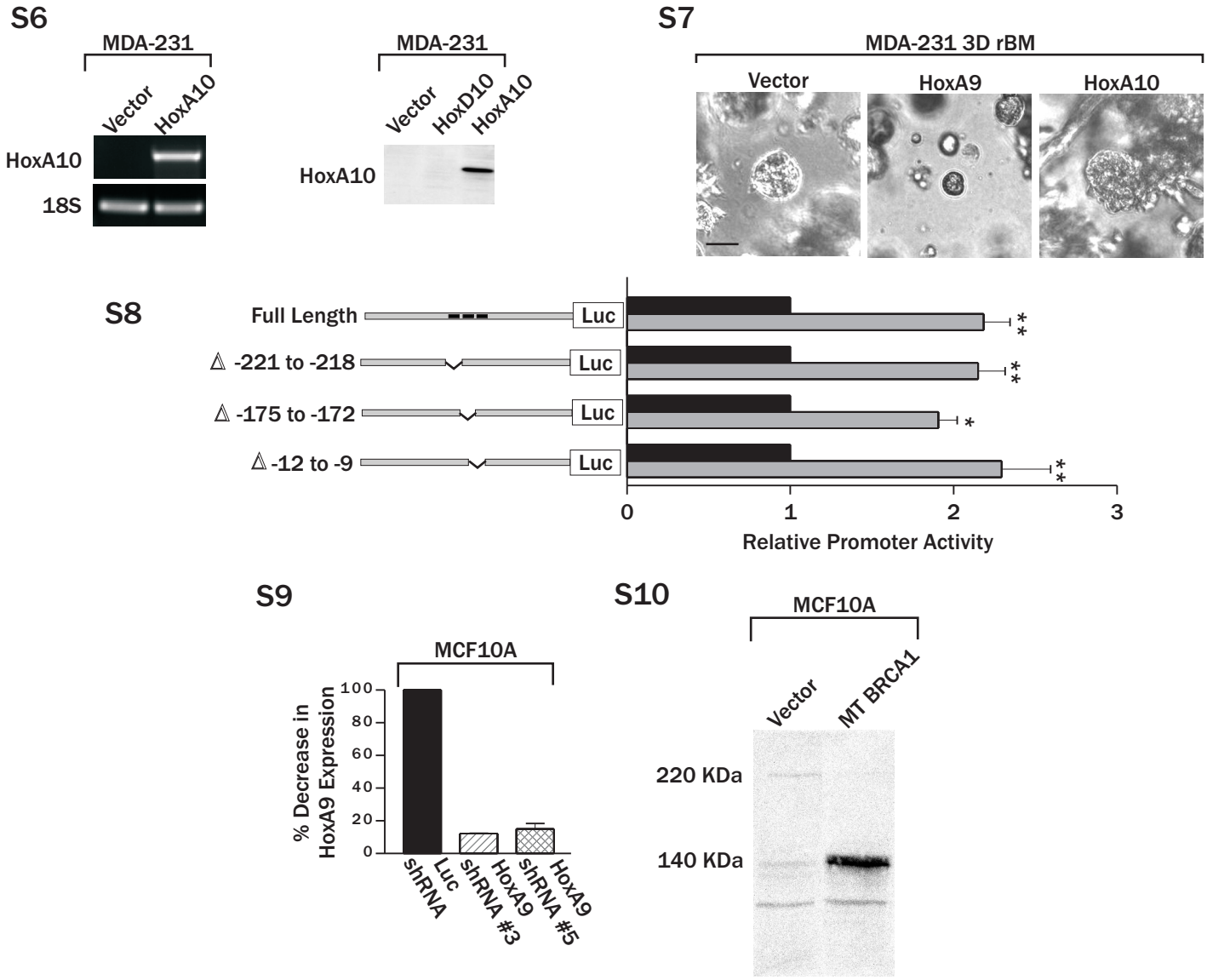

Supplemental Figure S6. Exogenous HoxA10 expression in MDA-231 breast tumor cells. Semi-Q-PCR gel (left) and immunoblot (right) showing levels of HoxA10 RNA and protein achieved upon re-expression in MDA-231 breast tumor cells. Lack of chemiluminescent signal in HoxD10 lysates demonstrates the specificity of the HoxA10 antibody.

Supplemental Figure S7. HoxA10 expression in mammary epithelial tumor cells does not reduce rBM colony growth. Phase contrast images of MDA-231 mammary epithelial tumor cells expressing a vector control, HoxA9 or HoxA10 transgene showing that growth inhibition within a 3D rBM is HoxA9 specific. Bar=50 μm.

Supplemental Figure S8. Mutational analysis of putative HoxA9 binding sites. Luciferase reporter analysis showing continued responsiveness of BRCA1 promoter constructs to addition of wild-type HoxA9 when single putative HoxA9 binding sites are deleted (Δ-221 to -218, Δ-175 to -172, and Δ-12 to -9) that is comparable to the activation of the full length BRCA1 promoter construct (compare gray bars). Data are normalized to matched vector control (black bars). Negative numbers refer to basepairs upstream of the BRCA1 transcription start site (9).

Supplemental Figure S9. shRNA mediated HoxA9 knockdown. Q-RT-PCR analysis of HoxA9 RNA levels in nonmalignant MCF10A mammary epithelial cells expressing a luciferase control shRNA construct (Luc) or a HoxA9 shRNA clone.

Supplemental Figure S10. The BRCA1 Δexon11b mutant functions as a dominant negative mutant. Immunoblot demonstrating that exogenous expression of BRCA1 Δexon11b (140KDa) in nonmalignant MCF10A cells completely abrogates levels of wild-type BRCA1 (220KDa) suggesting the BRCA1 mutant functions as a dominant negative.